

Sloshing-Induced Overflow Assessment of the Seismically-Isolated Nuclear Tanks

Kihyon Kwon, Hyun T. Park, Gil Y. Chung, Sang-Hoon Lee

Abstract—This paper focuses on assessing sloshing-induced overflow of the seismically-isolated nuclear tanks based on Fluid-Structure Interaction (FSI) analysis. Typically, fluid motion in the seismically-isolated nuclear tank systems may be rather amplified and even overflowed under earthquake. Sloshing-induced overflow in those structures has to be reliably assessed and predicted since it can often cause critical damages to humans and environments. FSI analysis is herein performed to compute the total cumulative overflowed water volume more accurately, by coupling ANSYS with CFX for structural and fluid analyses, respectively. The approach is illustrated on a nuclear liquid storage tank, Spent Fuel Pool (SFP), forgiven conditions under consideration: different liquid levels, Peak Ground Accelerations (PGAs), and post earthquakes.

Keywords—FSI analysis, seismically-isolated nuclear tank system, sloshing-induced overflow.

I. INTRODUCTION

IN recent years, the application of practical base isolation systems in nuclear power plants has become an important issue in aiming to preserve lifetime structural performance more safely in various seismic risk regions. In design phase, many requirements based on current specifications are imposed to avoid sudden structural and operating failures during the entire service life. Nevertheless, sloshing-induced failures in the seismically-isolated nuclear liquid storage tanks can be occurred under potential seismic loading. This is because the amplified sloshing due to a long-period shift can cause unexpected overflows of liquid which contains radioactive material. Accordingly, assessing and predicting sloshing behavior is required for successful implementation of the nuclear seismic isolation systems.

To date, numerous experimental and numerical studies have been performed to investigate liquid sloshing behavior [1]-[4]. However, these studies are limited to sloshing problems for the seismically non-isolated systems or non-nuclear structures. In the absence of reliable sloshing information on the seismically-isolated nuclear tank systems, accurate assessment and prediction of sloshing-induced overflow is not possible. In this study, sloshing assessment based on FSI approach is proposed. This approach is useful for quantifying the

time-variant sloshing height of liquid storage tanks as well as their sloshing-induced overflow [5]. In FSI analyses, interaction of structural elastic deformation and fluid motion is considered with flexible wall conditions not rigid. Three key parameters are used as important variables affecting the evaluation of the total cumulative overflowed water volumes: (i) different free surface levels (i.e., 65%, 75%, 85%, and 95.6% to tank height), (ii) different PGAs (0.3g, 0.4g, 0.5g, and 0.7g), and (iii) existence of post earthquakes (reduction in 25%, 50%, and 75% to PGA of 0.5g). The proposed approach is illustrated on a nuclear liquid storage tank, SFP, which is located in the auxiliary building. Floor acceleration time-histories, which are produced from the preliminary dynamic analysis for a full modeling of the nuclear auxiliary building, are applied to the tank base at each of the horizontal and vertical directions.

II. SLOSHING ASSESSMENT

A. Sloshing Assessment Based On FSI Analysis

Typically, liquid storage tanks can experience structural deterioration process due to violent sloshing even at very small amplitude excitations. In case of that seismic isolation systems are adopted, fluid motion becomes more fluctuated since the relative displacement between the base and top increases excessively. For this reason, sloshing assessment in those systems should be carried out.

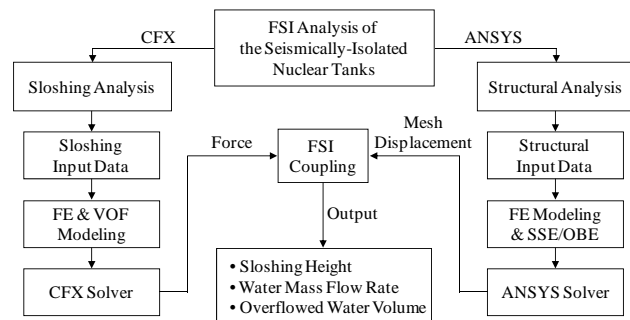


Fig. 1 Flowchart for FSI analysis

For the sloshing assessment, the inclusion of FSI effects is necessary to produce more reliable outputs. FSI analysis is commonly used to solve a multiphysics problem associated with the interaction between deformable structures and flow of fluid where it is filled internally or surrounded externally. The computational fluid dynamics (CFD) approach is also used to consider multiphase flow phenomena of gas/air and liquid [6]. As indicated in Fig. 1, FSI analysis is conducted by coupling two analytical solvers: (i) structural solver for mechanical

K. Kwon is with the Engineering Design Department, Korea Maintenance Co., Ltd., Seoul, Korea (phone: 82-2-830-7071; fax: 82-2-830-5256; e-mail: kik204@ kmctech.co.kr).

H. T. Park and G. Y. Chung are with the Engineering Design Department, Korea Maintenance Co., Ltd., Seoul, Korea (e-mail: defield@ kmctech.co.kr, cgy@ kmctech.co.kr).

S. Lee is with the Civil/Architectural Department, Korea Electric Power Corporation (KEPCO) Engineering & Construction Company, Yongin, Gyeonggi-Do, Korea (e-mail: shljrl@kepc0-enc.com).

application [7], and (ii) fluid solver for liquid sloshing [6]. All necessary boundary and loading conditions are imposed at the base of the tank for structural analysis. In the sloshing analysis, volume of fluid (VOF) method is employed due to its suitability for determining the shape and location of free surface [8]. Through the FSI coupling process, individual outputs including mesh displacement and force are continuously transferred to the structural and fluid solvers, respectively.

In this study, a two-way FSI analysis for sloshing assessment is performed by using common FE software programs ANSYS and CFX for structural and fluid analyses, respectively. Fluid motion is assumed to be ideally irrotational, incompressible, and inviscid.

B. FSI-Based Sloshing Verification

The 3D FSI approach adopted in this study was already validated in the former work conducted by the authors [5]. The computed sloshing height with flexible and rigid wall conditions was compared with the results of a 2D liquid storage steel tank (i.e., 9.14m by 6.10m) done by [9]. As shown in Fig. 2, the sloshing profiles agree well except the more increase in the peak sloshing height when the FSI analysis was performed with flexible wall condition.

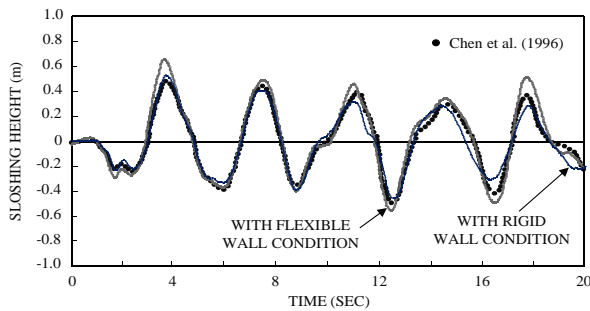


Fig. 2 FSI verification adapted from [5]

III. SLOSHING-INDUCED OVERFLOW

In an earthquake event, sloshing-induced overflow of liquid storage tanks can be occurred and well quantified by sloshing assessment based on FSI analysis. To estimate liquid overflow, mass flow rate has to be computed. It indicates the mass of a substance (e.g., fluid) passing through an identified surface per unit time. The mass flow rate, \dot{m} (kg/sec), at the opening boundary is defined as below [6]:

$$\dot{m}_i = \rho \cdot A_i \cdot V_i \quad (1)$$

where ρ is the mass density of the fluid, A is the cross-sectional area/surface, and V is the flow velocity of the mass elements, and i indicates the individual side walls in a rectangular tank (i.e., east, west, north, south).

Sloshing-induced overflow is estimated by dividing the computed mass flow rate in (1) into the fluid mass density. The total cumulative overflowed liquid volume, S_{total} (m^3), measured in four-side walls is given by:

$$S_{total} = \int_0^t \frac{\dot{m}_E(t) + \dot{m}_W(t) + \dot{m}_N(t) + \dot{m}_S(t)}{\rho} \cdot dt \quad (2)$$

where \dot{m}_E , \dot{m}_W , \dot{m}_N , and \dot{m}_S are the mass flow rate in each direction of SFP walls.

IV. APPLICATION

A. SFP Description

For performing sloshing-induced overflow assessment, a nuclear SFP, which is a pool-type rectangular reinforced concrete structure, is employed. SFP is typically 12.2m (40 ft) or more in depth with the bottom 4.3m (14 ft) equipped with storage racks which are designed to store spent fuel removed from nuclear reactors. It is operated to decrease the decay heat produced from spent fuel and to shield the radiation emitted. In this study, fluid filled in SFP of 12.80m (42 ft) deep is assumed to be water with free surface of 12.24m (40 ft 2 in). In addition, the effect of the storage racks on sloshing is investigated. All detailed information on SFP dimensions and material properties is presented in Table I.

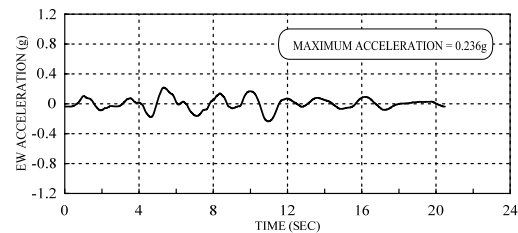
TABLE I
DIMENSIONS AND MATERIAL PROPERTIES

| Parameter | SFP | Fluid (Water) |
|------------------------------|-------|---------------|
| Width, W (m) | 10.52 | |
| Length, L (m) | 12.80 | |
| Height, H (m) | 12.80 | |
| Young's modulus, E (GPa) | 27.79 | |
| Poisson's ratio, ν | 0.17 | |
| Density, ρ (kg/m^3) | 2,403 | 997 |
| Free surface, h (m) | | 12.24 |

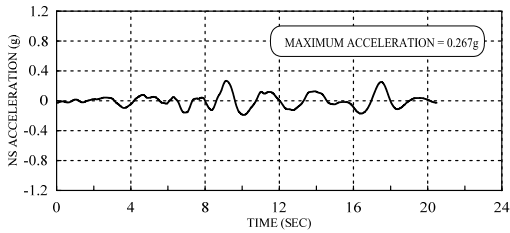
Dimensions indicate inner distance of SFP.

B. Seismic Loading

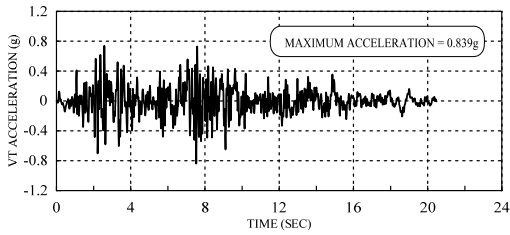
As described previously, PGA of 0.5g from the preliminary dynamic analysis was excited at bed rock level in order to produce floor acceleration time-histories at the isolated SFP base. As shown in Figs. 3 (a)-(c), the obtained acceleration inputs in FSI analysis are simultaneously applied to the base of SFP in east-west (EW), north-south (NS), and vertical (VT) directions.



(a) EW direction



(b) NS direction



(c) VT direction

Fig. 3 Acceleration time-histories for FSI analysis

C. FE Modeling of SFP and Racks

As a preliminary study, FSI analysis including fuel racks is performed to investigate their effect on SFP sloshing behavior. Accordingly, 3D FE modeling of SFP and fluid (i.e., water) is developed with the inclusion or exclusion of fuel racks by using the common software ANSYS and CFX, respectively [6], [7]. It is assumed that the fuel racks of 4.3m high extend to within 0.3m of the fuel pool walls with empty fuel cells. Rack-to-rack spacing is also ignored in this simplified model. Fig. 4 shows the typical dimensions of SFP and the layout of fuel racks. As mentioned previously, VOF model consisting of air and water regions is employed in liquid sloshing modeling, while solid model using element type of solid185 is developed in structural modeling.

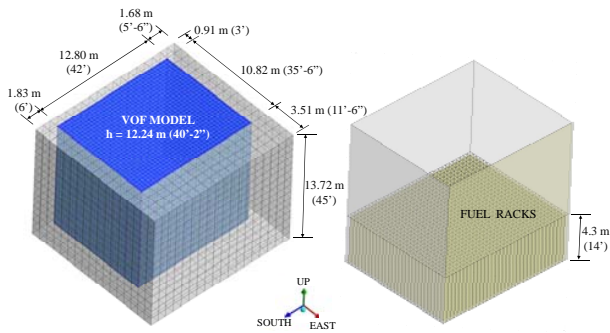
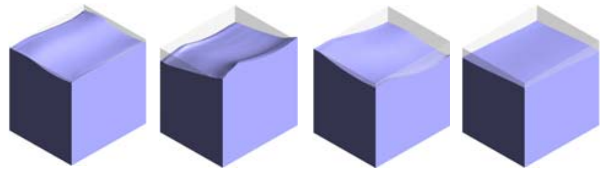


Fig. 4 FE modeling and dimensions

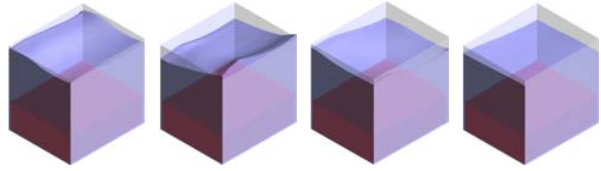
D. Sloshing Behavior and Overflow

Two-way FSI analyses for the SFP with or without fuel racks are conducted by imposing the acceleration excitations in all directions up to $t = 20.48$ sec (see Fig. 3).



(a) $t = 5$ sec (b) $t = 11.88$ sec (c) $t = 20.48$ sec (d) $t = 38$ sec

Fig. 5 Free surface profiles without fuel racks



(a) $t = 5$ sec (b) $t = 11.88$ sec (c) $t = 20.48$ sec (d) $t = 38$ sec

Fig. 6 Free surface profiles with fuel racks

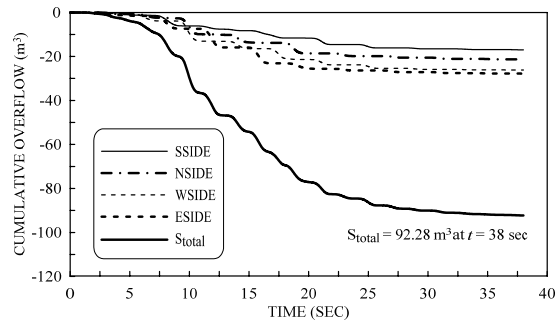


Fig. 7 Cumulative overflow profiles without fuel racks

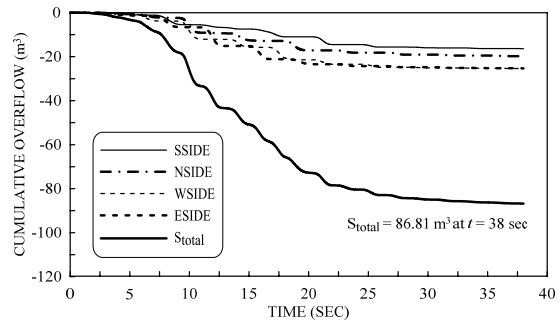


Fig. 8 Cumulative overflow profiles with fuel racks

The seismic excitations last $t = 38$ sec with zero excitations in order to make sloshing behavior converged stably. Figs. 5 and 6 show free surface profiles in both cases. Regardless of the inclusion of fuel racks, the peak sloshing height is occurred at $t = 11.88$ sec. It is observed that fluid motion in the SFP with fuel racks becomes a little gentler. The maximum and minimum cumulative overflows among four side walls are occurred in east and south walls, respectively (see Figs. 7 and 8). At $t = 38$ sec, the total cumulative overflows are 92.28 m^3 without racks and 86.81 m^3 with racks. The difference is not significant. Therefore, in the following case studies, fuel racks are not included in FSI modeling to improve computation efficiency

and produce more conservative outputs.

E. FSI Case Study

The total cumulative overflow of the SFP is assessed for the scenarios presented in Table II. Three FSI Cases considering free surface, PGA, and post earthquake are classified.

TABLE II
CASES FOR FSI ANALYSIS

| Cases | ID | Filled Water Level to SFP HEIGHT ^A (%) | PGA (g) | Aftershock Level to 0.5g PGA (%) |
|----------|-------|---|---------|----------------------------------|
| Case I | FWL65 | 65.0 | 0.5 | 0.0 |
| | FWL75 | 75.0 | 0.5 | 0.0 |
| | FWL85 | 85.0 | 0.5 | 0.0 |
| | FWL95 | 95.6 | 0.5 | 0.0 |
| Case II | PGA03 | 95.6 | 0.3 | 0.0 |
| | PGA04 | 95.6 | 0.4 | 0.0 |
| | PGA05 | 95.6 | 0.5 | 0.0 |
| | PGA07 | 95.6 | 0.7 | 0.0 |
| Case III | ASL00 | 95.6 | 0.5 | 0.0 |
| | ASL25 | 95.6 | 0.5 | 25.0 |
| | ASL50 | 95.6 | 0.5 | 50.0 |
| | ASL75 | 95.6 | 0.5 | 75.0 |

^ASFP Height, *H*, is 12.80 m.

Case I includes four different free surface levels with respect to SFP height, for given PGA of 0.5g with no aftershocks. Several PGAs (i.e., 0.3g, 0.4g, 0.5g, 0.7g) in Case II are taken into account as an excitation input, while different levels of aftershock are imposed in Case III.

F. Overflow Assessment

In Case I, sloshing-induced overflows of the SFP are computed by using (2) and plotted in Fig. 9. It is observed that the decrease in filled water levels (i.e., relatively lower free surface) leads to decrease in the total cumulative overflowed water volumes. In case of FWL65, S_{total} is considerably reduced around 90% as compared to that of FWL95. However, for practical design implementation, it is noted that FWLs 65, 75, and 85 except 95 (i.e., design free surface) have to be validated for their applicability associated with a safety margin of water level. In this context, finding the optimal free surface with the successful operation of the isolated SFP is challengeable.

For given free surface of 12.24m, different amplitudes of PGA (i.e., 0.3g, 0.4g, 0.5g, 0.7g) are excited at the SFP base up to $t = 38$ sec with no aftershocks. As shown in Fig. 10, the minimum sloshing-induced overflow is occurred in PGA03, whereas the maximum overflow is observed in PGA07 (i.e., PGA of 0.7g). The corresponding overflowed water volumes are presented in Table III, with the increase or decrease rate with respect to the reference PGA of 0.5g. Since liquid overflows in higher seismic risk can increase significantly, relevant actions for overflow prevention have to be taken in design and assessment phases of the isolated SFP.

FSI analyses including several aftershocks are performed in Case III, after fluid motion in the SFP is stabilized from the main shock of 0.5g. As an aftershock input, the scaled-down acceleration time-histories (i.e., ASL25, ASL50, ASL75) are imposed again from 38 sec to 58.48 sec, and then the SFP is

subjected to zero excitations up to 76sec. The associated overflow results are shown in Fig. 11 (see also Table III). With no aftershock (i.e., ASL00), the estimated overflow stays continuously constant. However, sloshing in other cases with a certain aftershock begins to fluctuate again after $t = 38$ sec. The additional overflowed volumes are 14.9m³, 25.3m³, and 36.7m³ in the cases ASL25, ASL50, and ASL75, respectively. The sloshing-induced overflow due to the aftershock is not relatively significant. This is reasonable because the actual free surface is already reduced during the previous main shock.

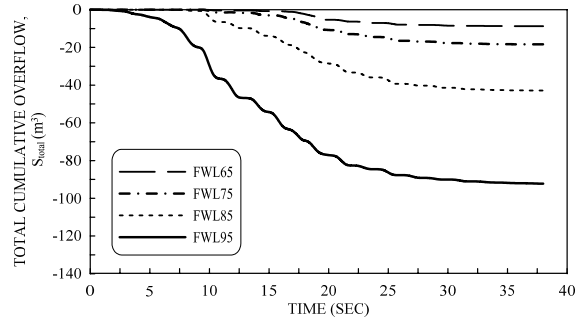


Fig. 9 Total cumulative overflow profiles according to different free surface levels without fuel racks (Case I)

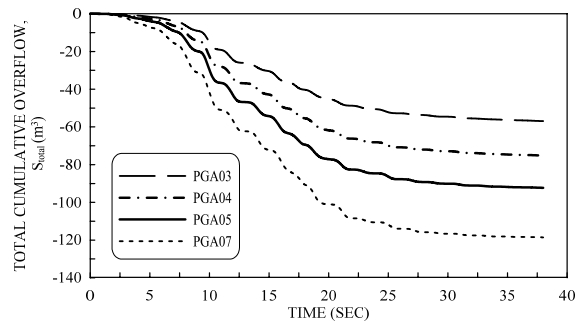


Fig. 10 Total cumulative overflow profiles according to different PGAs without fuel racks (Case II)

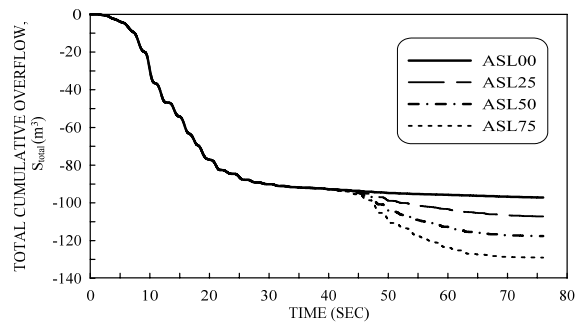


Fig. 11 Total cumulative overflow profiles according to different aftershocks without fuel racks (Case III)

TABLE III
TOTAL CUMULATIVE OVERFLOWS MEASURED AT THE IDENTIFIED TIME

| Cases | ID | $S_{total} (m^3)$ | | | Increase or decrease rate (%) |
|----------|--------------------|-------------------|--------------------|------------|-------------------------------|
| | | t = 20.48 sec | t = 38 sec | t = 76 sec | |
| Case I | FWL65 | 5.35 | 8.71 | - | (-)90.56 |
| | FWL75 | 10.89 | 18.35 | - | (-)80.11 |
| | FWL85 | 28.82 | 42.88 | - | (-)53.53 |
| | FWL95 ^a | 77.48 | 92.28 | - | RV |
| Case II | PGA03 | 45.89 | 56.90 | - | (-)38.34 |
| | PGA04 | 62.31 | 75.14 | - | (-)18.57 |
| | PGA05 ^a | 77.48 | 92.28 | - | RV |
| | PGA07 | 101.25 | 118.55 | - | (+)28.47 |
| Case III | ASL00 | 77.48 | 92.28 ^b | 97.13 | (+)5.26 |
| | ASL25 | 77.48 | 92.28 ^b | 107.18 | (+)16.15 |
| | ASL50 | 77.48 | 92.28 ^b | 117.62 | (+)27.46 |
| | ASL75 | 77.48 | 92.28 ^b | 129.00 | (+)39.79 |

^aFWL95 and PGA05 in cases I and II, respectively, are used as a reference value (RV) to compute the increase or decrease rate at the predefined time, $t = 38$ sec.

^b S_{total} at $t = 38$ sec is used as a RV to compute the increase rate at $t = 76$ sec.

V. CONCLUSION

This paper presents an approach for the sloshing-induced overflow assessment of the seismically-isolated nuclear SFP based on FSI analysis. From the analyses of the identified cases in this study, the following conclusions are drawn: (i) FSI technique can be effectively used to conduct reliable liquid overflow assessment of nuclear tanks; (ii) 3D FE modeling can be developed by linking ANSYS to CFX in terms of a tank structure and fluid, respectively; (iii) in a conservative way, fuel racks inside the SFP can be ignored in the sloshing-induced overflow assessment since their effect on sloshing is not significant; (iv) free surface can be considered as a very sensitive design factor associated with liquid overflow since its little reduction can lead to significant decrease in sloshing-induced overflow; (v) for same conditions except seismic loading, the higher PGA is, the more overflow increases; (vi) because of an aftershock that occurs after a previous large earthquake, additional liquid overflow can be more occurred, however, it depends on the remaining liquid level after the main shock; and (vii) further research is needed for finding optimal design solutions to prevent unexpected liquid overflows in the seismically-isolated nuclear tanks.

ACKNOWLEDGMENT

The support to Korean Maintenance Co., Ltd., from Korea Electric Power Corporation (KEPCO) Engineering & Construction Company Inc., under award 2011T100200078 associated with the project "Development and Engineering of Practical Base Isolation System for Nuclear Power Plant Export" is gratefully acknowledged. The opinions and conclusions presented in this paper are those of the writers and do not necessarily reflect the views of the sponsoring organization.

REFERENCES

- [1] P. K. Malhotra, "Method for seismic base isolation of liquid-storage tanks," *Journal of Structural Engineering*, vol. 123, no. 1, pp. 113-116, Jan. 1997.
- [2] H. W. Shenton III, and F. P. Hampton, "Seismic response of isolated elevated water tanks," *Journal of Structural Engineering*, vol. 125, no. 9, pp. 965-976, Sep. 1999.
- [3] Y. H. Chen, W. S. Hwang, and C. H. Ko, "Sloshing behaviors of rectangular and cylindrical liquid tanks subjected to harmonic and seismic excitations," *Earthquake Engineering and Structural Dynamics*, vol. 36, pp. 1701-1717, 2007.
- [4] M. De Angelis, R. Giannini, and F. Paolacci, "Experimental investigation on the seismic response of a steel liquid storage tank equipped with floating roof by shaking table tests," *Earthquake Engineering and Structural Dynamics*, vol. 39, pp. 377-396, 2010.
- [5] K. Kwon, H. T. Park, G. Y. Chung, and S. Lee, "Baffle effects of the seismically-isolated nuclear tanks on sloshing reduction based on FSI analysis," in *Proc. 22ndSMiRT Conf.*, San Francisco, 2013, Paper ID 1004.
- [6] Ansys, Inc., "ANSYS CFX-Pre User's Guide Release 13.0," Canonsburg, PA, 2010.
- [7] Ansys, Inc., "Theory Reference for ANSYS and ANSYS Workbench Release 13.0," Canonsburg, PA, 2010.
- [8] M. A. Goudarzi, and S. R. Sabbagh-Yazdi, "Investigation of nonlinear sloshing effects in seismically excited tanks," *Soil Dynamics and Earthquake Engineering*, vol. 43, pp. 653-669, 2012.
- [9] W. Chen, M. A. Haroun, and F. Liu, "Large amplitude liquid sloshing in seismically excited tanks," *Earthquake Engineering and Structural Dynamics*, vol. 25, pp. 653-669, 1996.